Jurnal Riset Kimia

ISSN (print) : 1978-628X
ISSN (online) : 2476-8960

Hydrothermal and Coprecipitation Synthesis Design of $BiVO_4$ for Methylene Blue Degradation

Anung Riapanitra[1], Tien Setyaningtyas[1], Michael Julian Haryanto[1,2], Ghinatanitha Haqqu Haryadinaru[1*]

[1]Department of Chemistry, Natural Science Faculty, Jenderal Soedirman University, Indonesia
[2]Graduate School of Science and Engineering, University of Toyama, Japan

Corresponding Author:
Ghinatanitha Haqqu Haryadinaru
ghinatanitha02@gmail.com

Received: July 2024
Accepted: February 2025
Published: March 2025

Abstract

This study investigated the characteristics and photocatalytic activity of $BiVO_4$ photocatalyst synthesized using hydrothermal and coprecipitation methods for methylene blue (MB) degradation under visible light. The variation of synthesis parameters, including pH, calcination temperature, and pH of MB solution, affects the crystal structure, morphology, and photocatalytic efficiency of the material. XRD characterization results show that the hydrothermal method produces $BiVO_4$ with pure scheelite(m-s) monoclinic phase and high crystallinity, while the coprecipitation method produces a combination of scheelite(m-s) monoclinic and orthorhombic $Bi_4V_2O_{11}$ phases, which contributes to enhanced photocatalytic activity through better charge separation. The average crystal size of the hydrothermal method is 17.85 nm, larger than that of coprecipitation (11.41-14.71 nm), which gives the coprecipitated material a surface area advantage. SEM analysis showed rod-like morphology in hydrothermal, while coprecipitation produced sphere-grape-like particles. UV-Vis DRS results show that hydrothermal synthesized $BiVO_4$ has a band gap energy of 2.28 eV, smaller than BiV(4)(400) (2.46 eV) and higher than BiV(4)(550) (2.07 eV) synthesized using coprecipitation method. This smaller band gap energy indicates that the interaction of Bi^{3+} and VO_4^{3-} ions in the hydrothermal material is better, thus favoring visible light absorption. The highest photocatalytic activity was obtained from the coprecipitated material with a degradation efficiency of 89.32% at pH 11 within 150 min, higher than the hydrothermal material which reached 76.06% under similar conditions. This photocatalytic activity was dominated by OH^* and O_2^{-*} radicals, which play a role in MB degradation. This study shows that designing synthesis pH parameters (4-7), calcination temperature (400℃), and coprecipitation method produced a material with optimum photocatalytic performance, making $BiVO_4$ a superior candidate for colored wastewater treatment applications.

Keywords: *bismuth vanadate, hydrothermal, coprecipitation, methylene blue, photocatalyst design, adsorption*

Introduction

Indonesia is experiencing significant economic growth in various sectors, including the textile, pulp, and food industries[1]. Positive socioeconomic impacts have resulted from this. However, a rise in wastewater runoff to the environment containing synthetic dyes such as methylene blue (MB) has emerged as a negative impact. MB is a hardly biodegraded compound

DOI: https://doi.org/ 10.25077/jrk.v16i1.740

usually used in textile industries and is dangerous when introduced to the surrounding ecosystems[2]. As its constituent, aromatic benzene is carcinogenic and mutagenic, leading to severe environmental issues for an extended period. Therefore, water MB contamination will cause a serious issue that requires immediate action to minimize ecological loss and socioeconomic costs that may result.

Indonesia is also blessed geographically. It is situated in the equatorial region, receiving energy from the sun year-round, which is beneficial for photocatalyst application, a combination of catalysis and light energy to degrade organic pollutants[3]. One of the promising photocatalytic materials recently being developed is Bismuth vanadate ($BiVO_4$)[4], [5]. $BiVO_4$ is applicable under visible light radiation, making it a low activation energy and environmentally friendly material. $BiVO_4$ has three crystal morphologies: tetragonal zircon (t-z), monoclinic scheelite (m-s), and tetragonal scheelite (t-s), with band gap energies ranging from 2.4 to 2.9eV. The m-s morphology is thermodynamically more stable than the t-z[6]. Additionally, the m-s and t-z morphologies are prospective to p-n junction reactions, where they can produce electron-hole photogeneration[7]. Notably, the photocatalytic reaction happens on the material surface, suggesting that many factors, such as particle size and morphology, regulate photocatalytic activity. Amorphous nanostructure $BiVO_4$ (m-s) and crystalline $BiVO_4$ (t-z) can form at room temperature. According to Huo et al. (2017), an irreversible transition from crystalline (t-z) to crystalline (m-s) occurs at calcination temperatures more than 400°C[8]. Therefore, it is essential to design the material to increase its photocatalytic activity, durability, and reusability especially using chemical methods such as the hydrothermal process which is environmentally friendly.

$BiVO_4$ (m-s) is usually synthesized using the hydrothermal technique, which requires high temperatures for a period of time[9]. On the other hand, the coprecipitation technique is the easiest of several fabrication processes and does not require such a large amount of energy and a long time[10]. Although many have designed $BiVO_4$ synthesis processes through hydrothermal, research comparing the coprecipitation method with hydrothermal for $BiVO_4$ synthesis is still limited[11], [12], [13]. Therefore, this study aims to design $BiVO_4$ material by varying pH reaction, calcination temperature, and parameter of the MB solution. Material synthesized using the coprecipitation will be compared with the hydrothermally synthesized $BiVO_4$ to understand the effect of particle size, morphology, and crystal structure on the photocatalytic degradation process of MB under visible light.

Experimental

Materials

The materials used in the study include ammonium metavanadate (NH_4VO_3) p.a., bismuth (III) nitrate pentahydrate ($Bi(NO_3)_3.5H_2O$) p.a., nitric acid (HNO_3) 2M p.a., sodium hydroxide (NaOH) 2M p.a., demineralized water, distilled water, MB dye, acidifier (HCl) and base (NaOH), absolute ethanol, benzoquinone, isopropanol, ammonium oxalate, and filter paper.

Instruments

The tools used in the research include glassware, stirring rod, spatula, magnetic stirrer, analytical balance, calcining furnace, oven, centrifuge, desiccator, UV-visible spectrophotometer Shimadzu 1800, scanning electron microscope (SEM) JEOL JSM-6520LA, X-ray diffraction (XRD) Shimadzu XRD-7000, UV-visible diffuse reflectance spectroscopy (UV-Vis DRS) JASCO V-670, and a visible light reactor.

Methods

Synthesis of $BiVO_4$ by Coprecipitation

The synthesis of $BiVO_4$ was performed based on the methods developed by Ganeshbabu (2020) and Guo et al. (2017)[10], [14]. A total of 0.001 mol (0.485 g) of $Bi(NO_3)_3$-$5H_2O$ was dissolved in 8 mL of 2M HNO_3 solution,

forming solution A. Separately, 0.001 mol (0.117 g) of NH_4VO_3 was dissolved in 8 mL of 2M NaOH solution using a magnetic stirrer at room temperature for 30 min, forming solution B. Solution B was then slowly added (dropwise) to solution A while stirring. Solution B was then slowly added (dropwise) to solution A while stirring. After mixing, the pH of the solution was adjusted to a specific value (4, 7, or 10) by adding acid or base as needed. The stirring process was continued for 3 hours under dark conditions using a closed reactor. At the end of the process, the solution was centrifuged to separate the precipitates. The precipitate obtained was washed three times with demineralized water (aqua DM) and absolute ethanol to remove the remaining solution. The precipitates were then dried in an oven at 70°C for 4 hours. The dried precipitates were then calcined at different temperatures (not calcined (NC), 300℃, 350℃, 400℃, 450℃, 500℃, and 550℃ for 2 hours in a furnace.

Hydrothermal Synthesis of $BiVO_4$

$BiVO_4$ was synthesized using a method adapted from the work of Mansha et al. (2023)[15]. A total of 4.3863 g $Bi(NO_3)_3$-$5H_2O$ was dissolved in 100 mL of distilled water to form the first solution, while 0.3509 g NH_4VO_3 was dissolved in 100 mL of distilled water to form the second solution. The two solutions were then slowly mixed with continuous stirring for 1 hour using a magnetic stirrer. After mixing, the pH of the solution was adjusted to 10 by gradually adding 2.5 M NaOH solution while stirring continuously for 30 minutes. The mixture was then placed in an autoclave and heated at 180°C for 14 hours. After the hydrothermal process, the mixture was centrifuged to separate the precipitates. The resulting precipitates were filtered and washed three times with ethanol and demineralized water to remove the remaining reaction solution. The clean precipitates were then dried at 60℃ for 24 hours. Next, the sample was calcined at 400℃ for 4 hours to improve the crystal quality and stability.

Optimum pH Optimization of Coprecipitated $BiVO_4$ Photocatalysts

A total of 0.05 g of $BiVO_4$ photocatalyst from coprecipitation synthesis with pH variations of 3, 7, and 11 was added to a glass beaker containing 50 mL of 10 ppm MB solution at pH 11. The solution was stirred at 600 rpm under dark conditions at room temperature for 30 min to achieve adsorption-desorption equilibrium. The mixture was then irradiated under visible light for 2.5 h. Samples of ± 5 mL were taken at each 30-minute interval, then diluted twice and centrifuged. The absorbance of the solution was measured using a UV-Vis spectrophotometer at the maximum wavelength. From the results of this measurement, the pH of the photocatalyst with the highest percentage of degradation can be determined.

Table 1. Photocatalyst Design Variation

Hydrothermal Material Design	pH Value (x)						Controlled	Denotation
BiV	4		7		10		Calcination temperature (400°C)	BiV(x)
Coprecipitation Material Design	Calcination temperature (℃) (y)						Controlled	Denotation
BiV	300	350	400	450	500	550	pH Value (x)	BiV(x)(y)

DOI: https://doi.org/ 10.25077/jrk.v16i1.740

ISSN (print) : 1978-628X
ISSN (online) : 2476-8960

Calcination Temperature Optimization of Coprecipitated $BiVO_4$ Photocatalysts

A total of 0.05 g of $BiVO_4$ photocatalyst from coprecipitation synthesis with different calcination temperatures of 300, 350, 400, 450, 500, and 550℃ at the optimum pH was added to a glass beaker containing 50 mL of 10 ppm MB solution at pH 11. The solution was stirred at 600 rpm in the dark at room temperature for 30 minutes to reach adsorption-desorption equilibrium. The solution was then exposed to visible light for 2.5 hours. Samples of ±5 mL were taken every 30 minutes, then diluted twice and centrifuged. The absorbance of the solution was measured using a UV-Vis spectrophotometer at the maximum wavelength. Based on these measurements, the calcination temperature of the photocatalyst, which gives the maximum percentage of degradation, can be determined.

Determination of Optimum pH of Methylene Blue Solution

0.1 g of the synthesized $BiVO_4$ photocatalyst was added to 50 mL of 10 ppm MB solution at different pH values, namely 3, 5, 7, 9, and 11. The solution was stirred under dark conditions and at room temperature for 30 minutes, and then irradiated under visible light for 2.5 hours. After 2.5 hours, ± 5 mL samples were taken, and the absorbance was measured using a UV-visible spectrophotometer at the maximum wavelength.

Photocatalytic Degradation Mechanism of $BiVO_4$

A 0.1 g of $BiVO_4$ photocatalyst in the optimum condition with the highest dye degradation % was added to 50 mL of 10 ppm MB solution at pH 11. Then, 0.2 mL of 0.25 M benzoquinone solution was added. The solution was stirred for 30 minutes in the dark at room temperature, then irradiated for 2.5 hours under visible light. Samples were taken (±5) and centrifuged to measure absorbance. The procedure was repeated using 4 μL isopropanol PA scavenger and 0.2 mL 0.25 M ammonium oxalate scavenger.

Results and Discussion

Crystal Structure of $BiVO_4$

The crystal structure of synthesized materials using coprecipitation method at various pH is provided in **Figure 1**. $BiVO_4$ (m-s) and orthorhombic $Bi_4V_2O_{11}$ are formed at all pH values (JCPDS No. 00-014-0688) and (JCPDS No. 00-040-0940)[10], [11], [16]. Dominant peaks at 19, 28.5, 29, 30.5, and 34.5 with their respective crystal plane ([011], [130], [121], [040], and [200]) characterize $BiVO_4$ (m-s). However, the striking peak at 32.2 may explain the crystal plane of orthorhombic $Bi_4V_2O_{11}$. $Bi_4V_2O_{11}$ is a bismuth-based material with a layered structure that favors charge separation and enhanced photocatalytic efficiency[17].

Under acidic conditions, only small $BiVO_4$ nuclei are formed, which may result in a more stable amorphous m-s than the t-z. Adding NaOH facilitates the transition of crystalline $BiVO_4$ (m-s) from crystalline $BiVO_4$ (t-z)[6]. This transition is essential for enhancing the material's structural and functional properties. Within the pH range of 4–7, highly crystalline composite bismuth materials are formed, which exhibit significant potential for photocatalytic applications due to their improved light absorption and charge separation capabilities. In addition, at pH 10, a more composite-like material is associated with bismuth, vanadate, oxynitrate, and subnitrate species. This is possibly due to the aggregation of cationic Bi^{3+}, which may form various polymers. The compounds Bi_2O_3 (JCPDS No. 01-074-1633) and Bi_7VO_{13} (JCPDS No. 00-044-0322) are bismuth vanadate species that can form under alkaline conditions, which are suspected to reduce the photocatalytic activity of the material[18]. In addition, **Figure 2** shows the crystal structure of $BiVO_4$ synthesized with hydrothermal method. $BiVO_4$ (m-s) can be seen from the diffraction patterns at 28.5, 28.9, and 30.6, corresponding to the crystal plane [130], [121], and [040]. All the sharp diffraction patterns indicate a high

DOI: https://doi.org/ 10.25077/jrk.v16i1.740

crystal nature with an m-s structure, and the results agree with the reference[11].

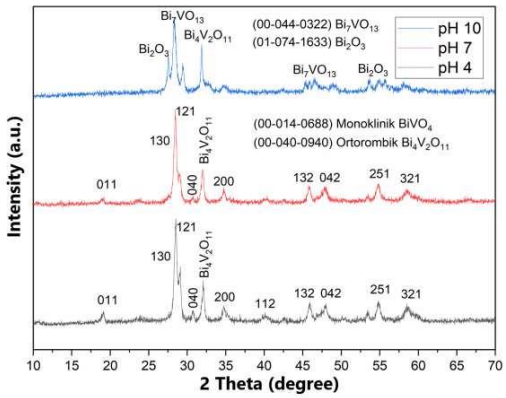

Figure 1. The crystal structure of $BiVO_4$ synthesized with coprecipitation at pH 4, 7, and 10

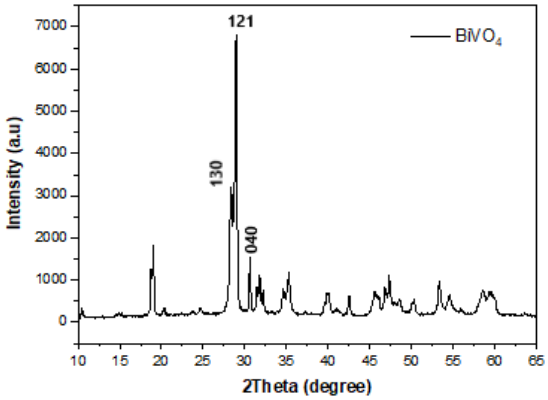

Figure 2. The crystal structure of $BiVO_4$ synthesized with hydrothermal

$BiVO_4$ crystal structure synthesized with hydrothermal appears to have higher crystallinity as shown by the peak intensity.

From the XRD results, the crystalline size of the samples can be obtained using the Debye Scherrer theorem as follows:

$$D = \frac{k\,\lambda}{\beta\,cos\,\theta}$$

Where D is the crystalline size (nm), λ is the wavelength of X-ray (1.54056Å), k is a constant of 0.94, β is the FWHM (Full Width at Half Maximum) value, and θ is the investigated diffraction angle. The average crystalline sizes of BiV(4)(400), BiV(7)(400), BiV(10)(400), and BiV(4)(550) are 14.71, 14.51, 12.74, and 11.41 nm, respectively. Meanwhile, the hydrothermal method produces a larger crystal size of 17.85 nm. The smaller crystal size from coprecipitation provides the advantage of a larger surface area, which is important for enhancing photocatalytic reactivity.

Band Gap Energy of $BiVO_4$

UV-VIS DRS was employed to identify the photochemical properties of $BiVO_4$. The band gap energy of a semiconductor material is a crucial parameter that determines its optical and electronic properties. The absorption spectra and band gap energy profiles are provided in **Figure 3**. The results indicate that the BiV(4)(400) and BiV(4)(550) samples have bandgap energies of 2.46 eV and 2.07 eV,

DOI: https://doi.org/ 10.25077/jrk.v16i1.740

respectively. All the materials exhibit photocatalytic activity in the visible light region, with an absorption edge around 580 nm, and agree with $BiVO_4$ (m-s) characteristics. The BiV(4)(550) shows a weaker absorption profile before 500 nm but improved absorption beyond 500 nm, possibly due to the formation of a heterostructure phase (M-T) caused by the increase in calcination temperatures, which decreases the intensity of several redox sites ([011], [121])[19]. A heterostructure phase in BiV(4)(550) causes the band gap energy to be smaller than the BiV(4)(400). However, a weaker absorption profile before 500 nm indicates that redox sites in BiV(4)(550) are not as many as in BiV(4)(400). The atomic structure of the $BiVO_4$ becomes unstable as the calcination temperature increases. In BiV_4O_{11} with heterostructures (m-s) and (t-z), p-n junction activity occurs under visible light irradiation. The interfacial interaction between the two structures facilitates electron and hole migration, leading to the photogeneration of charge carriers[20].

The hydrothermal method tends to produce materials with more ordered crystals and more stable structures compared to the coprecipitation method. In hydrothermal $BiVO_4$, the monoclinic scheelite (m-s) structure is more dominant, and it usually has a smaller band gap due to better interaction between Bi and V ions in the crystal structure. This interaction can reduce the distance between the conduction band and the valence band, reducing the bandgap value of the material (2.28 eV). Overall, although the band gap of hydrothermal $BiVO_4$ is slightly larger than that of BiV(4)(550), the differences in morphology and crystalline phase still result in differences in photocatalytic performance.

Morphological Structure of BiVO4

Identifying the morphological structure of the material aims to understand the surface properties, size, and shape of the particles. A rod-like shape is formed in the $BiVO_4$ sample synthesized by hydrothermal. In contrast, a homogeneous sphere-grape-like particle with a smooth surface is observed in the $BiVO_4$ sample synthesized with coprecipitation (**Figure 4**).

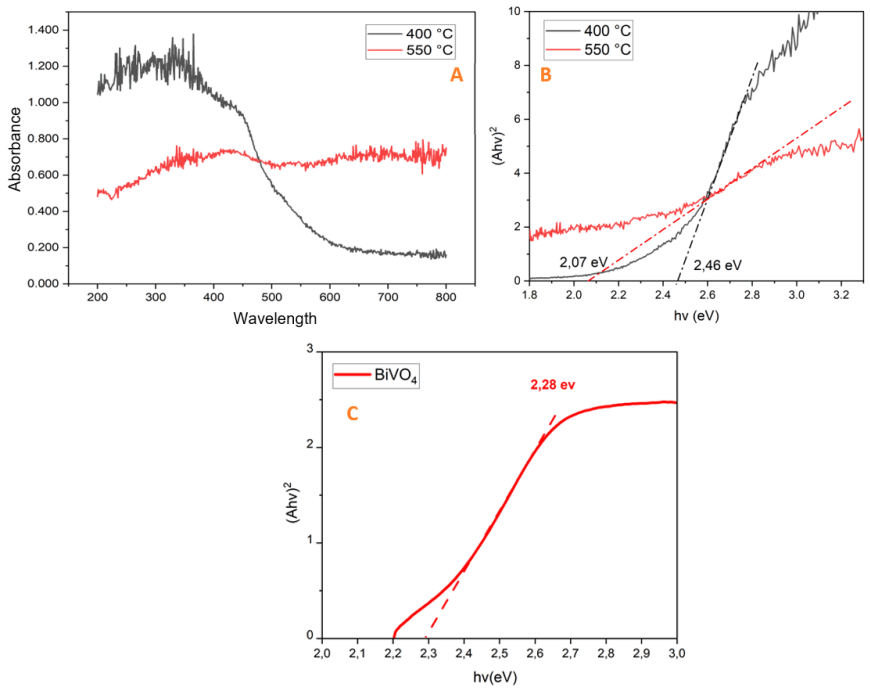

Figure 3 (A) Absorbance spectra and (B) Tauc plot of coprecipitated BiV(4)(400) and BiV(4)(550). The Tauc plot of hydrothermal $BiVO_4$ is also presented in panel (C).

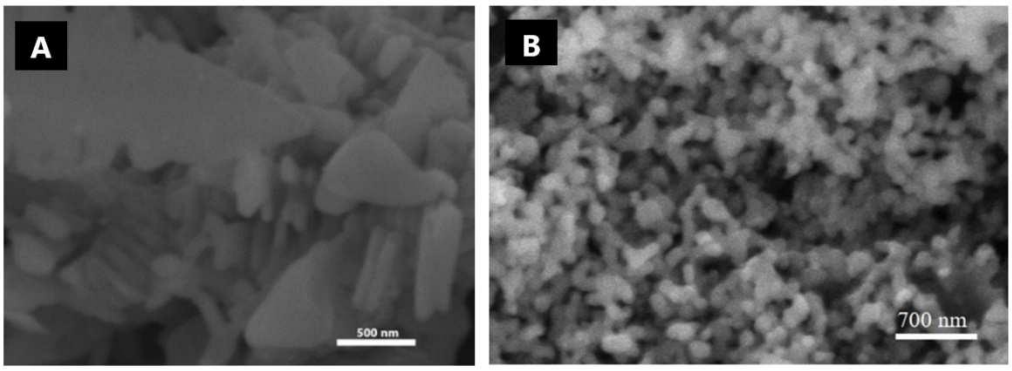

Figure 4. Morphology results of $BiVO_4$ synthesized with (A) hydrothermal and (B) coprecipitation with the magnification of 25000 and 20000 times, respectively.

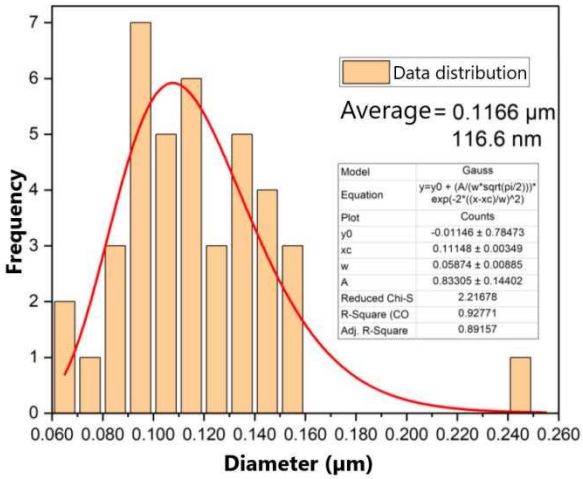

Figure 5. Crystal size distribution of BiV(4)(400), manually measured using ImageJ software

The hydrothermal synthesis process at 180°C followed by calcination at 400°C creates ideal conditions for forming this morphology. High hydrothermal temperature accelerates the reaction kinetics and crystal growth, while calcination increases crystallinity and removes organic residues. During the hydrothermal process, Bi^{3+} and VO_4^{3-} ions interact effectively and form crystal nuclei, which grow anisotropically, creating a rod-like morphology. Further calcination improves the crystal structure and reduces defects. The agglomeration of rod-like particles occurs due to the interaction of Van der Waals and electrostatic forces, as well as the tendency of nanoparticles to reduce surface energy[21].

The inhibition of solvent diffusion into the material's inner structure can cause the formation of granules and porous nanostructures. This follows previous studies, such as those that produced SEM images of sphere shapes with smooth surfaces through the coprecipitation method at a calcination

DOI: https://doi.org/ 10.25077/jrk.v16i1.740

temperature of 400°C[8, 22]. From the SEM imagery, physical particle size can be measured. An average of 116.6 nm with a distribution from 60-260 nm (n = 40) was obtained, indicating a nanoscale size of particles (**Figure 5**).

Optimum pH and Calcination Temperature for $BiVO_4$ Coprecipitation

The synthesis pH and calcination temperature in the $BiVO_4$ coprecipitation process were identified to optimize the material characteristics that affect its photocatalytic activity. These parameters play a role in determining the crystalline structure, particle size, and material distribution, which directly affect the charge transfer efficiency in the methylene blue (MB) degradation process under visible light.

The effect of coprecipitation synthesis pH on the photocatalytic activity of $BiVO_4$ in **Figure 6** shows significant variation, with the highest activity achieved at pH 4 (71.66%), followed by pH 10 (48.59%) and pH 7 (31.64%). At pH 4, a crystalline monoclinic-scheelite (m-s) phase is formed, and the presence of $Bi_4V_2O_{11}$, identified through XRD data, increases the photocatalytic efficiency by inhibiting electron-hole pair recombination[23]. SEM results show a more dispersed particle morphology and smaller particle size at this pH, thus enlarging the active surface area and allowing more efficient interaction between the photocatalyst and MB molecules. In contrast, at pH 7, the photocatalytic activity decreased drastically due to mineralization by NaOH, which led to the loss of crystal peaks and reduced redox sites such as [011] and [121]. At pH 10, although the activity was higher than that at pH 7, supersaturation of the solution triggered the formation of particle aggregation, which decreased the active surface area and adsorption efficiency. The predominant semicrystalline phase at pH 10 may also limit charge transfer compared to the crystalline phase at pH 4[24].

Calcination temperature also has a significant effect on the characteristics of $BiVO_4$. **Figure 7** shows that at 400°C, the photocatalytic activity reaches a peak (74.56%) due to the formation of a thermodynamically stable monoclinic-scheelite (m-s) phase, with dominant [010] and [121] facets that provide more redox sites for electron-hole transfer. UV-Vis DRS analysis confirmed maximum absorption in the visible light region at this temperature, thus supporting the degradation efficiency of MB. However, at temperatures above 400°C, there is a decrease in activity due to sintering and particle agglomeration, which reduces the active surface area and oxidation-reduction sites, although the visible light uptake remains good[25]. Overall, combining synthesis pH 4 and calcination temperature 400°C produced $BiVO_4$ with optimal crystalline structure, particle size, and photocatalytic properties for MB degradation.

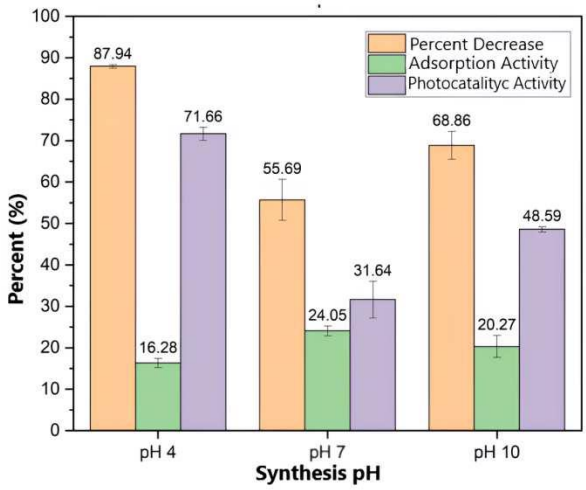

Figure 6. Effect of Coprecipitation Synthesis pH Parameters on Methylene Blue Degradation

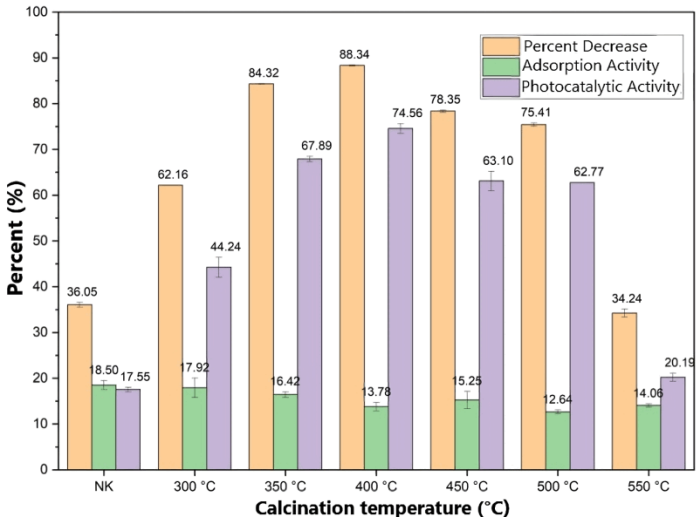

Figure 7. Effect of Calcination Temperature on Coprecipitation Synthesis Method on Methylene Blue Degradation

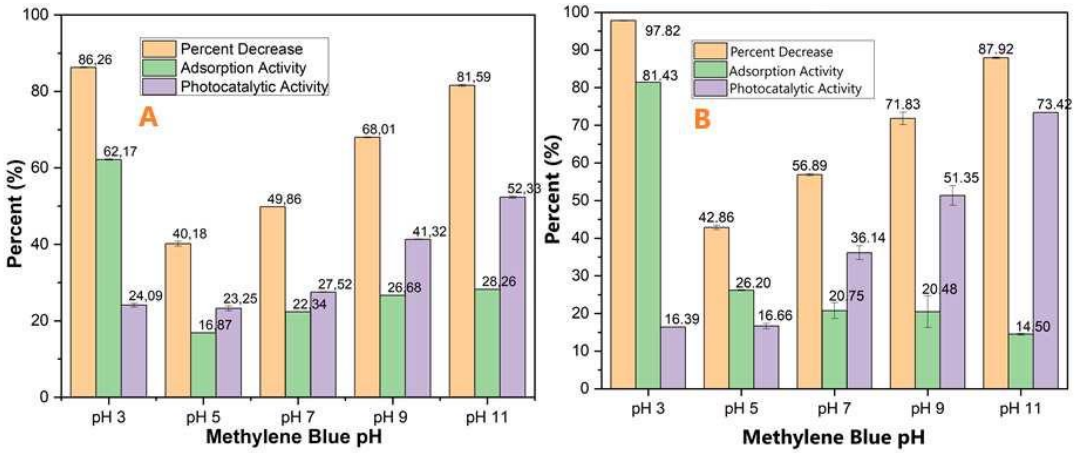

Figure 8. Graph of % adsorption activity, photocatalytic activity and degradation of Hydrothermal (A) and Coprecipitated (B) $BiVO_4$ against MB degradation

Identification of Optimum pH of MB

Based on **Figure 8A**, the hydrothermally synthesized $BiVO_4$ material shows the highest adsorption activity at pH 3 of 62.17%, which decreases significantly as the pH value increases until it reaches 28.26% at pH 11. This phenomenon is in accordance with the electrostatic properties of the material. At pH < pHpzc (3.46), the surface of the material is positively charged due to protonation, so the interaction with anions from MB becomes very strong[26]. However, at pH > pHpzc, the material surface becomes negatively charged due to deprotonation by OH^- ions, which causes electrostatic repulsion and reduces adsorption activity[27]. The photocatalytic activity of the hydrothermal material increased with increasing basicity, reaching the highest value at pH 11 of 52.33%. This is due to the high concentration of OH^- ions at alkaline pH,

DOI: https://doi.org/ 10.25077/jrk.v16i1.740

which favors the formation of hydroxyl radicals (•OH) through oxidation by holes (h^+).

In **Figure 8B**, the $BiVO_4$ material from coprecipitation synthesis shows a similar pattern but with higher adsorption and photocatalytic activity values. The highest adsorption occurred at pH 3 with 81.43%, while at pH 11, the adsorption value decreased to 20.48%.

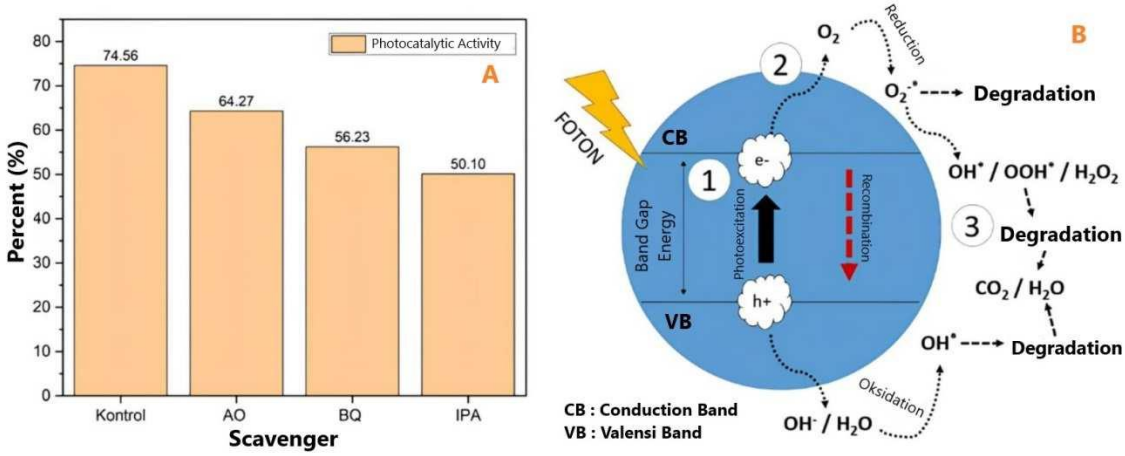

Figure 9. (A) Photocatalytic species of $BiVO_4$ and (B) its schematic photocatalytic mechanism

Like the hydrothermal material, the change in the surface charge of the material due to the pHpzc value affects the adsorption activity[28]. The coprecipitated material had the highest value of 73.42% for photocatalytic activity at pH 11. The abundant OH^- concentration at alkaline pH promotes the formation of •OH radicals active in the MB degradation.

Photocatalytic Mechanism of $BiVO_4$

The photocatalytic mechanism was tested by observing the changes in MB degradation values after adding scavengers. The scavengers used included ammonium oxalate to test the catalytic function of holes, benzoquinone for superoxide radicals (O_2^-), and isopropanol for hydroxyl radicals (OH). **Figure 9** shows that the photocatalytic degradation of MB is dominated by •OH radicals, as seen from the most significant decrease in degradation values with the addition of isopropanol. Holes in the valence band oxidize H_2O or adsorbed OH^- ions to produce •OH radicals. This is reinforced by the system conditions at basic pH (11), where OH^- ions are more easily oxidized by holes into •OH radicals[29].

The benzoquinone scavenger showed a decrease in the photocatalytic activity value, indicating that the treatment of synthesis parameters affected the position of the Muliken electronegativity energy, thereby increasing the material's ability to produce radicals, especially O_2^{-*} radicals. The addition of scavengers decreased photocatalytic activity because the scavengers captured the resulting radicals, reducing the number of radicals that played a role in MB degradation[30].

It can be concluded that the photocatalytic activity by $BiVO_4$ is dominated by the presence of OH^* and O_2^{-*} radicals (**Figure 9**). OH^* and O_2^{-*} radicals are the most dominant ROS radicals in photocatalysis. This O_2^{-*} radical can undergo further reactions in acid to form OH^*, OOH^*, and H_2O_2 radicals with smaller photocatalytic activities[31].

Conclusions

$BiVO_4$ photocatalysts synthesized via hydrothermal and coprecipitation methods showed good performance in methylene blue degradation. The coprecipitation method

yielded superior degradation efficiency (89.32%) thanks to the combination of monoclinic scheelite and orthorhombic phases and smaller crystal sizes, increasing the active surface area. In contrast, the hydrothermal method produced material with higher crystallinity and smaller band gap energy (2.28 eV) while maintaining visible light range absorption, although the degradation efficiency was lower (76.06%) due to the larger crystal size. The photocatalytic activity of both methods was dominated by OH^* and O_2^{-*} radicals, with optimal results at pH 11 and calcination temperature of 400℃. Thus, $BiVO_4$ has excellent potential for colored wastewater treatment applications through photocatalyst technology.

Acknowledgment

Jenderal Soedirman University supported this study under "Unsoed Research Grant" No. 27.157/UN23.37/PT.01.03/II/2023.

References

1. N. W. Yuningrat, N. Retug, I. M. Gunamantha, J. Analis, and K. Fmipa, "Fotodegradasi Methyl Orange Dalam Reaktor Fixed Bed Batu Apung-Semen", (2016).
2. N. Andriana, "Pemanfaatan Silika Gel Berbasis Abu Terbang (*Fly Ash*) Batubara PLTU Paiton-Probolinggo Sebagai Adsorben Zat Warna Metilen Biru," Universitas Jember, Jember, (2016).
3. M. N. Chong, B. Jin, C. W. K. Chow, and C. Saint, "Recent developments in photocatalytic water treatment technology: A review," *Water Res*, 44 (10): (2010), doi: 10.1016/j.watres.2010.02.039.
4. A. Riapanitra, T. Setyaningtyas, and G. H. Haryadinaru, "Photodegradation of Methylene Blue Dye Using $BiVO_4$/g-C_3N_4 Composites under Visible Light Irradiation," *Jurnal Kimia Sains dan Aplikasi*, **27 (8)**: (2024), doi: 10.14710/jksa.27.8.363-370.
5. A. Riapanitra, T. Setyaningtyas, K. Riyani, R. Andreas, A. L. Ariyanti, and U. Sulaeman, "Synthesis of vanadium oxide material and its photocatalytic activity in the degradation of methylene blue," 2022, p. 020007. doi: 10.1063/5.0103707.
6. G. Tan, L. Zhang, H. Ren, S. Wei, J. Huang, and A. Xia, "Effects of pH on the Hierarchical Structures and Photocatalytic Performance of $BiVO_4$ Powders Prepared via the Microwave Hydrothermal Method," *ACS Appl Mater Interfaces*, **5(11):** 2013, doi: 10.1021/am401019m.
7. B. Baral, K. H. Reddy, and K. M. Parida, "Construction of M-BiVO4/T-BiVO4 isotype heterojunction for enhanced photocatalytic degradation of Norfloxacine and Oxygen evolution reaction," *J Colloid Interface Sci*, **554:** 278–295 (2019), doi: 10.1016/j.jcis.2019.07.007.
8. R. Huo, X.-L. Yang, Y.-Q. Liu, and Y.-H. Xu, "Visible-light photocatalytic degradation of glyphosate over BiVO 4 prepared by different co-precipitation methods," *Mater Res Bull*, **88**: 56–61 (2017), doi: 10.1016/j.materresbull.2016.12.012.
9. C. Wang *et al.*, "Comparison of highly active Type-I and Type-II heterojunction photocatalytic composites synthesized by electrospinning for humic acid degradation," *Chem Phys Lett*, **803:** 139815 (2022), doi: 10.1016/j.cplett.2022.139815.
10. M. Ganeshbabu, N. Kannan, P. S. Venkatesh, G. Paulraj, K. Jeganathan, and D. MubarakAli, "Synthesis and characterization of BiVO 4 nanoparticles for environmental applications," *RSC Adv*, **10 (31):** 18315–18322 (2020), doi: 10.1039/D0RA01065K.
11. Z. Qu, P. Liu, X. Yang, F. Wang, W. Zhang, and C. Fei, "Microstructure and Characteristic of BiVO4 Prepared under Different pH Values: Photocatalytic Efficiency and Antibacterial Activity," *Materials*, **9(3):** 129 (2016), doi: 10.3390/ma9030129.

 DOI: https://doi.org/ 10.25077/jrk.v16i1.740

12. H. Jiang *et al.*, "Hydrothermal fabrication and visible-light-driven photocatalytic properties of bismuth vanadate with multiple morphologies and/or porous structures for Methyl Orange degradation," *Journal of Environmental Sciences*, **24(3):** 449–457 (2012), doi: 10.1016/S1001-0742(11)60793-6.

13. Y. K. Kshetri *et al.*, "Microwave hydrothermal synthesis and upconversion properties of BiVO 4 nanoparticles," *Nanotechnology*, **31(24):** 244001 (2020), doi: 10.1088/1361-6528/ab78ae.

14. M. Guo, Q. He, A. Wang, W. Wang, and Z. Fu, "A Novel, Simple and Green Way to Fabricate $BiVO_4$ with Excellent Photocatalytic Activity and Its Methylene Blue Decomposition Mechanism," *Crystals (Basel)*, **6(7):** 81 (2016), doi: 10.3390/cryst6070081.

15. M. S. Mansha *et al.*, "Facile hydrothermal synthesis of $BiVO_4$ nanomaterials for degradation of industrial waste," *Heliyon*, **9(5):** e15978 (2023), doi: 10.1016/j.heliyon.2023.e15978.

16. M. Arumugam and M. Y. Choi, "Effect of Operational Parameters on the Degradation of Methylene Blue Using Visible Light Active $BiVO_4$ Photocatalyst," *Bull Korean Chem Soc*, **41(3):** 304–309 (2020), doi: 10.1002/bkcs.11972.

17. Z. Jiang *et al.*, "One-Pot Solvothermal Synthesis of Bi4V2O11 as A New Solar Water Oxidation Photocatalyst," *Sci Rep*, **6(1):** 22727 (2016), doi: 10.1038/srep22727.

18. M. Han, "$BiVO_4$-based nanoparticles for visible light photocatalytic applications," Nanyang Technological University, 2014. doi: 10.32657/10356/59858.

19. D. Yusefah, A. Jurusan, K. Fmipa, F. Matematika, D. Ilmu, and P. Alam, "The Effect of Calcination Temperature On The Crystal Size And The Band Gap Energy TiO_2-SiO_2 Composites, (2014).

20. L. Zhang *et al.*, "Efficient removal of methylene blue over composite-phase BiVO4 fabricated by hydrothermal control synthesis," *Mater Chem Phys*, **136(2–3):** 897–902 (2012), doi: 10.1016/j.matchemphys.2012.08.016.

21. B. Guan *et al.*, "Review on Synthesis, Modification, Morphology, and Combination of $BiVO_4$ -based Catalysts for Photochemistry: Status, Advances, and Perspectives," *Energy & Fuels*, **38(2):** 806–853 (2024), doi: 10.1021/acs.energyfuels.3c03932.

22. T. Duy Nguyen *et al.*, "Synthesized $BiVO_4$ was by the co-precipitation method for Rhodamine B degradation under visible light," *IOP Conf Ser Mater Sci Eng*, **542(1):** 012058 (2019), doi: 10.1088/1757-899X/542/1/012058.

23. A. B. Baunsele and H. Missa, "Kajian Kinetika Adsorpsi Metilen Biru Menggunakan Adsorben Sabut Kelapa," *Akta Kimia Indonesia*, **5(2):** 76, Nov. 2020, doi: 10.12962/j25493736.v5i2.7791.

24. F. Ambrosio, J. Wiktor, and A. Pasquarello, "pH-Dependent Surface Chemistry from First Principles: Application to the $BiVO_4$ (010)–Water Interface," *ACS Appl Mater Interfaces*, **10(12):** 10011–10021 (2018), doi: 10.1021/acsami.7b16545.

25. T. Sharifi *et al.*, "Tailored $BiVO_4$ for enhanced visible-light photocatalytic performance," *J Environ Chem Eng*, **9(5):** 106025 (2021), doi: 10.1016/j.jece.2021.106025.

26. P. Hemmatpour and A. Nezamzadeh-Ejhieh, "A Z-scheme CdS/BiVO4 photocatalysis towards Eriochrome black T: An experimental design and mechanism study," *Chemosphere*, **307:** (135925) (2022), doi: 10.1016/j.chemosphere.2022.135925.

27. A. I. Moral-Rodríguez *et al.*, "Novel and green synthesis of $BiVO_4$ and GO/$BiVO_4$ photocatalysts for efficient dyes degradation under blue LED illumination," *Ceram Int*, **48(1):** 1264–1276 (2022), doi: 10.1016/j.ceramint.2021.09.211.

28. P. K. Panda, R. Pattanaik, S. Mishra, D. Pradhan, and S. Kumar Dash, "Superior photocatalytic degradation of MB dye

using $BiVO_4$ nanoparticles under solar light irradiation," *Mater Today Proc*, (2023), doi: 10.1016/j.matpr.2023.11.039.

29. T. Soltani, A. Tayyebi, and B.-K. Lee, "$BiFeO_3/BiVO_4$ p–n heterojunction for efficient and stable photocatalytic and photoelectrochemical water splitting under visible-light irradiation," *Catal Today*, **340:** 188–196 (2020), doi: 10.1016/j.cattod.2018.09.030.
30. A. Lebedev, F. Anariba, X. Li, and P. Wu, "Rational design of visible-light-sensitive Ag-$BiVO_4$ oxides by matching redox potentials of catalyst, dyes, and reactive oxygen species towards more efficient photocatalytic degradation," *J Environ Chem Eng*, **8(3):** 103748 (2020), doi: 10.1016/j.jece.2020.103748.
31. O. Monfort and G. Plesch, "Bismuth vanadate-based semiconductor photocatalysts: a short critical review on the efficiency and the mechanism of photodegradation of organic pollutants," *Environmental Science and Pollution Research*, 25(20): 19362–19379 (2018), doi: 10.1007/s11356-018-2437-9.

 DOI: https://doi.org/ 10.25077/jrk.v16i1.740